AGU PUBLICATIONS

Geophysical Research Letters

RESEARCH LETTER
10.1002/2014GL060934

Key Points:
- Observations reveal missing sources of MSA over the tropical Pacific
- The unknown sulfur source has large impacts on aerosol formation and climate

Supporting Information:
- Readme
- Table S1 and Figures S1–S7

Correspondence to:
Y. Zhang,
yuzhong.zhang@eas.gatech.edu

Citation:
Zhang, Y., Y. Wang, B. A. Gray, D. Gu, L. Mauldin, C. Cantrell, and A. Bandy (2014), Surface and free tropospheric sources of methanesulfonic acid over the tropical Pacific Ocean, *Geophys. Res. Lett.*, *41*, doi:10.1002/2014GL060934.

Received 21 JUN 2014
Accepted 30 JUN 2014
Accepted article online 1 JUL 2014

Surface and free tropospheric sources of methanesulfonic acid over the tropical Pacific Ocean

Yuzhong Zhang[1], Yuhang Wang[1], Burton Alonza Gray[1], Dasa Gu[1,2], Lee Mauldin[3,4], Christopher Cantrell[3], and Alan Bandy[5,6]

[1]School of Earth and Atmospheric Sciences, Georgia Institute of Technology, Atlanta, Georgia, USA, [2]Now at Atmospheric Chemistry and Meteorology, Pacific Northwest National Laboratory, Richland, Washington, USA, [3]Department of Atmospheric and Oceanic Sciences, University of Colorado Boulder, Boulder, Colorado, USA, [4]Department of Physics, University of Helsinki, Helsinki, Finland, [5]Chemistry Department, Drexel University, Philadelphia, Pennsylvania, USA, [6]Deceased 24 December 2011

Abstract The production of sulfate aerosols through sulfur chemistry in marine environments is critical to the tropical climate system. However, not all sulfur compounds have been studied in detail. One such compound is methanesulfonic acid (MSA). In this study, we use a one-dimensional chemical transport model to analyze the observed vertical profiles of gas phase MSA during the Pacific Atmospheric Sulfur Experiment. The observed sharp decrease in MSA from the surface to 600 m implies a surface source of 4.0×10^7 molecules/cm^2/s. Evidence suggests that this source is photolytically enhanced in daytime. We also find that the observed large increase of MSA from the boundary layer into the lower free troposphere (1000–2000 m) results mainly from the degassing of MSA from dehydrated aerosols. We estimate a source of 1.2×10^7 molecules/cm^2/s to the free troposphere through this pathway. This source of soluble MSA could potentially provide an important precursor for new particle formation in the free troposphere over the tropics, affecting the climate system through aerosol-cloud interactions.

1. Introduction

Critical to the tropical climate system is the production of sulfate through organic sulfur emission and oxidation in marine environments [e.g., *Charlson et al*., 1987]. Since the discovery that dimethyl sulfide (DMS) is emitted in large quantities from the ocean [*Barnard et al*., 1982], marine sulfur chemistry has been studied extensively. The oxidation of DMS is mainly by the hydroxyl radical (OH), which converts more than half of DMS to sulfur dioxide (SO_2) [*Davis et al*., 1998, 1999; *Chen et al*., 2000; *Wang et al*., 2001]. Further oxidation of SO_2 in the gas or aerosol phase produces sulfuric acid (H_2SO_4), which can either condense onto existing particles or form new particles under favorable conditions [*Davis et al*., 1999; *Mauldin et al*., 1999; *Weber et al*., 2001]. In addition to SO_2 and H_2SO_4, marine sulfur chemistry also involves other sulfur-containing compounds such as dimethyl sulfoxide (DMSO), methane sulfinic acid (MSIA), and methanesulfonic acid (MSA). These species, although believed to be important, have not been studied as extensively as DMS and SO_2.

Extensive airborne measurements on board the NSF/National Center for Atmospheric Research (NCAR) C130 aircraft were carried out to study sulfur chemistry and its interaction with dynamics during the Pacific Atmospheric Sulfur Experiment (PASE) over the tropical Pacific (in the vicinity of Christmas Island, 157°20′W, 1°52′N) in August and September of 2007. Vertical distributions of a relatively complete set of sulfur-containing compounds, including DMS, SO_2, H_2SO_4, and MSA, were measured, providing observational constraints to test our understanding of sulfur chemistry in the marine boundary layer (MBL) and lower free troposphere (LFT) over tropical regions. Using the one-dimensional version of the Regional chEmical trAnsport Model (1-D REAM), *Gray et al*. [2011] showed that the modeled vertical profiles of DMS and SO_2 during the PASE are in reasonable agreement with observations. They estimated an average DMS-to-SO_2 conversion efficiency of 73%. However, the budget analysis by *Faloona et al*. [2009] using PASE measurements found a close to unity conversion efficiency from DMS to SO_2. *Bandy et al*. [2011] suggested that the discrepancy might be an indication of an unknown sulfur source, whose strength is approximately half that for DMS. In this

©2014. American Geophysical Union. All Rights Reserved.

work, we analyze the vertical distributions of MSA measured during PASE to understand its sources and transport over the tropical Pacific.

2. Data and Model Description

2.1. PASE Aircraft Data

During PASE, 14 research flights using the NSF/NCAR C-130 took place. Extensive aircraft measurements were obtained in the marine boundary layer (down to ~50 m), the buffer layer (BuL, 600–1300 m), and the lower free troposphere (up to 2000 m), providing well-resolved vertical profiles from the ocean surface to ~2000 m. The sampling strategy and flight patterns are described in *Conley et al*. [2009] and *Faloona et al*. [2009]. As in the work by *Gray et al*. [2011], our analysis used only Flights 2, 3, 5, 8, 11, and 12. We excluded Flight 7 because of short sampling duration. Flights 1, 9, and 10 were excluded because of incomplete measurement data. We also eliminated Flight 4 because it was a cloud-sampling mission. We did not include the two nighttime flights (6 and 13) in our analysis because of our research focus in daytime chemistry. A more detailed discussion concerning the choice of flights can be found in *Gray et al*. [2011].

In this study, we make use of the full suite of PASE measurements such as aerosol size distribution and concentrations of MSA, DMS, SO_2, OH, CO, O_3, and water vapor. MSA was measured with selected-ion chemical-ionization mass spectrometry (SICIMS) [*Mauldin et al*., 1999]. Dry aerosol size distributions were measured using a combination of HiGEAR differential mobility analyzer, optical particle counter, and aerodynamic particle sizer instrumentation [*Clarke et al*., 2004]. To account for the uptake of water at ambient relative humidity [*Bandy et al*., 2011], we applied a humidity correction on the aerosol size distribution and used corrected values to calculate aerosol scavenging. DMS measurements were taken by atmospheric-pressure ionization mass spectrometers [*Bandy et al*., 2002], OH was measured with selected-ion chemical-ionization mass spectrometry (SICIMS) [*Mauldin et al*., 1998], and O_3 was recorded using a fast chemiluminescence instrument [*Ridley et al*., 1992]. Readers can refer to *Bandy et al* [2011] for more information on the PASE measurements.

2.2. Model Description

Previously, we have applied the 1-D REAM to investigate polar photochemistry at the South Pole [*Wang et al*., 2007], urban photochemistry in China [*Liu et al*., 2010, 2012], and sulfur chemistry over the tropical Pacific [*Gray et al*., 2011]. In this work, we use the 1-D REAM, which incorporates modules for O_3-NO_x-hydrocarbon photochemistry, marine sulfur chemistry, cloud/aerosol scavenging, turbulent and convective transport, and dry/wet deposition, to analyze the vertical distribution and sources of MSA over the tropical Pacific. The sulfur chemistry module utilizes a condensed sulfur chemistry mechanism involving gas phase species of DMS, SO_2, H_2SO_4, DMSO, $DMSO_2$, MSIA, and MSA [*Chen et al*., 2000]. To test the possible impact of BrO, we also include the reaction between DMS and BrO in the mechanism. Kinetic data of the reactions are updated following *Zhu et al*. [2006] (Table S1 in the supporting information). Aerosol scavenging rate constant is calculated based on measured aerosol size distribution (see supporting information for details). Vertical transport is simulated using meteorological fields assimilated by the Weather Research and Forecasting (WRF) model based on the National Centers for Environmental Prediction reanalysis data. To simulate marine sulfur chemistry, near-surface DMS concentrations are specified as the observed values, and model simulated DMS profiles are in good agreement with the observations [*Gray et al*., 2011]. We scale the simulated OH profile to match the observations and use the scaled values for sulfur chemistry calculation. In addition, observed concentrations of CO, O_3, and water vapor are also used to constrain the model. For each flight, we run the model in a 1 min time step repeatedly using the chemical constraints and meteorological fields of that day for a period of 30 days to achieve a quasi–steady state, and only the results of the last day are used for analysis.

Gray et al. [2011] have shown that the 1-D REAM with such setups is able to reproduce the observed vertical profiles and daytime variations of DMS and SO_2 during the PASE (Figure S1 in the supporting information). In this study, we use the model by *Gray et al*. [2011], referred to as the BASE simulation, as the starting point of our analysis. Recognizing that the BASE simulation cannot fully describe the observed vertical profile of MSA, we design several exploratory simulations with varying model configurations (Table 1). To investigate the sharp gradient near the surface, we specify in the near-surface layer MSA as observed, BrO as 2 pptv and

©2014. American Geophysical Union. All Rights Reserved.

Table 1. Simulations Conducted With the 1-D REAM in This Study

Name	Description
BASE	A 1-D REAM simulation follows *Gray et al.* [2011]. All other simulations are based on this simulation.
FIX	MSA in the bottom layer is specified to the observations.
BrO	BrO in the bottom layer is fixed at 2 pptv.
DMSO	DMSO in the bottom layer is fixed at 4 pptv.
NOSCAV	Aerosol scavenging is turned off in the LFT.
DEGAS DF10/DF20	Aerosol scavenging is turned off in the LFT. In addition, a fraction of MSA is degassed from fine-mode aerosols if relative humidity is $< 40\%$. Aerosol-phase MSA originates from scavenged MSA and MSA produced from scavenged DMSO and MSIA. We conducted two DEGAS simulations with degassing fractions (DF) of 10% and 20%, denoted as DEGAS DF10 and DEGAS DF20, respectively.

DMSO as 4 pptv, respectively, in the FIX, BrO, and DMSO simulations. To explore the cause of the enhancement of MSA in the LFT, we turn off aerosol scavenging in the LFT in the NOSCAV simulation. We further allow MSA to degas from aerosols in the DEGAS simulation, in which aerosol-phase MSA is treated as a tracer and degassing takes place when relative humidity is lower than 40%. The aerosol-phase MSA includes MSA either directly scavenged by aerosols or rapidly produced in aqueous phase from scavenged DMSO and MSIA [*Zhu et al.*, 2006].

3. Results and Discussion

3.1. MSA Gradient in the MBL

One of the remarkable features revealed in the PASE data is a pronounced negative gradient of MSA from the ocean surface to ~600 m. Unlike well-mixed SO_2 [*Gray et al.*, 2011], the observed median MSA concentrations decrease rapidly in the MBL, from 2.1×10^6 molecules/cm^3 near the ocean surface to 0.6×10^6 molecules/cm^3 at 600 m (Figure 1). This change in concentrations translates to a negative gradient of 2.5×10^6 molecules/cm^3/km in the MBL. The BASE simulation, with chemical production from DMS oxidation being the only MSA source, fails to reproduce the gradient and significantly underestimates MSA concentrations in the lower MBL (Figure 1). The discrepancy between simulated and observed vertical profiles implies a missing MSA source close to the ocean surface that is not included in the BASE simulation.

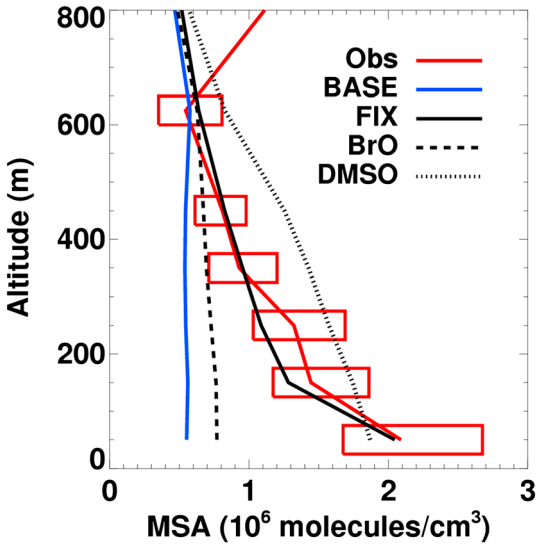

Figure 1. Observed and simulated daytime median vertical profiles of MSA in the MBL. Observational data are represented with red solid lines. Red boxes indicate inner quartiles. Model results from BASE, FIX, BrO, and DMSO simulations are shown with blue solid, black solid, black dashed, and black dotted lines, respectively.

Constrained with observed MSA concentrations at the surface layer, the FIX simulation is able to reproduce both the concentrations and the gradient of MSA in the MBL (Figure 1), supporting the idea that an additional surface source can explain the discrepancy between the observations and BASE simulation. The budget calculation of the FIX simulation indicates a missing source of 4.0×10^7 molecules/cm^2/s (Figure 3), which is much stronger than the estimated chemical production from DMS oxidation (9.0×10^6 molecules/cm^2/s). The comparison between daytime and before-dawn measurements (Figure S2 in the supporting information) implies that this source is photolytically enhanced in daytime. However, we cannot conclusively determine the nature of this source using only the observations from PASE. We therefore explore several possible mechanisms with the aid of the 1-D model.

©2014. American Geophysical Union. All Rights Reserved.

One possible explanation is the oxidation of DMS by BrO, which is not modeled in the BASE simulation. Since the DMS + BrO reaction is through the addition channel, which favors MSA production, it is plausible that the DMS + BrO reaction contributes to the missing source of MSA. Previous studies on the PASE (e.g., *Gray et al.* [2011]) found that based on SO_2 simulations, they could not either prove or rule out the presence of BrO in the MBL at a level of 1 pptv. To test the impact of BrO on MSA production, we assume in the BrO simulation the daily maximum BrO mixing ratio at the ocean surface to be 2 pptv. The BrO simulation results in the additional chemical production of MSA of 1.0×10^6 molecules/cm^2/s. This addition, however, is insignificant in comparison to the missing source of 4.0×10^7 molecules/cm^2/s and is unable to sustain the negative gradient in the MBL (Figure 1). Therefore, we conclude that the presence of BrO, if any, is unlikely to be the primary reason for the missing source of MSA.

Another possible reason for the underestimation of MSA production can be uncounted for sources of MSA precursors such as DMSO. Unexpected high levels of DMSO (10–50 pptv) have been previously reported over the tropical ocean [*Bandy et al*., 1996; *Nowak et al*., 2001]. Although DMSO measurements are unfortunately unavailable in the PASE, we are able to test the impact of high DMSO concentrations on MSA production with the model. In the DMSO simulation, we fix surface DMSO at 4 pptv, a moderately high concentration [*Nowak et al*., 2001]. The enhanced DMSO concentrations increase the chemical production of MSA to 4.9×10^7 molecules/cm^2/s, which is comparable to the strength of the missing source. However, the median vertical gradient of MSA from the DMSO simulation appears to be smaller than observations (Figure 1). The gradient is not maintained in the model because DMSO is vertically mixed in the MBL, and the resulting MSA production from DMSO is not limited to the surface layer (as in the FIX case), leading to a model overestimate in most of the MBL. Despite imperfect agreement between the simulated and observed gradients, the results underscore the potential role of DMSO in MSA production. To further test this hypothesis, future studies require concurrent measurements of DMSO and MSA.

In addition to unidentified chemistry, another possible explanation for the missing source of MSA is a primary emission directly from the ocean. This explanation is supported by the correlation between MSA concentrations and wind speeds in lower altitudes ($<$200 m) (Figure S3). However, this correlation can also be a signal that MSA is being produced from very reactive sulfur species emitted from the ocean. Furthermore, because MSA is far more soluble than DMS (Henry's law constant is 10^{15} for MSA and 0.5 mol kg^{-1} atm^{-1} for DMS), it cannot easily degas from the water surface, unless aided by other mechanisms such as a thin organic film at the surface of the ocean, in which MSA is moderately soluble.

3.2. MSA Increase in the LFT

The vertical profile of MSA observed during PASE features a large increase in the LFT. The average mixing ratio of MSA in the LFT is 2.2×10^7 molecules/cm^3, 1 order of magnitude larger than that in the MBL (Figure 2a). Similar features of enhanced MSA in the free troposphere are also found in the data from the Pacific Exploratory Missions-A (PEM-A) and PEM-B campaigns [*Davis et al*., 1999; *Mauldin et al*., 1999] (Figure S4 in the supporting information). Analyses of measurements show that the controlling factor of the MSA concentrations in the LFT is humidity. Figure 2 also shows that MSA concentrations are negatively correlated with relative humidity (RH) in the LFT during PASE. Similar relationships between MSA and RH in the LFT are also found in PEM-A and PEM-B data (Figure S4 in the supporting information).

The BASE simulation fails to reproduce MSA enhancement in the LFT. Recognizing that the affinity of gaseous MSA to aerosols is mainly due to its high solubility and that aerosols in the dry LFT tend to lose their water content, we perform the NOSCAV simulation, in which we turn off aerosol scavenging in the LFT. With the NOSCAV simulation, the model is able to generate a peak at the right altitude (~2 km), but the magnitude (0.7×10^7 molecules/cm^3 at 2 km) is still much smaller than the observations (an average of 2.2×10^7 molecules/cm^3 at 2 km) (Figure 2a). Model analysis shows that to reproduce the observed magnitude would require a source of MSA in the LFT at ~1.2×10^7 molecules/cm^2/s (Figure 3).

We hypothesize that the source of MSA in the LFT is degassing from aerosols as a result of high vapor pressure in the dry LFT. Previous experiments showed that the vapor pressure of MSA increases rapidly as the concentration of the solution increases (about 10 ppbv at 40 mol/L, see Figure S5 in the supporting information) [*Covington et al*., 1973; *Hoppel*, 1987]. To maintain equilibrium, MSA tends to degas from dehydrated aerosols in the dry LFT, which constitutes a nonnegligible source of MSA in the LFT.

©2014. American Geophysical Union. All Rights Reserved.

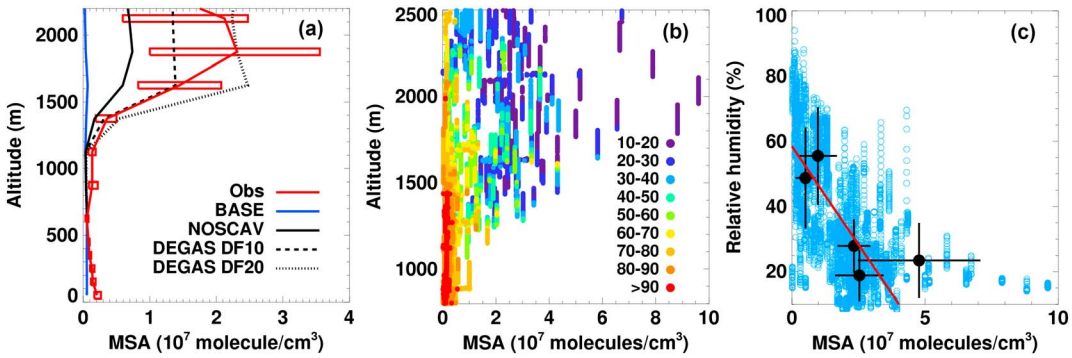

Figure 2. (a) Observed and simulated daytime median vertical profiles of MSA from surface to 2000 m. Observational data are represented with red lines. Red boxes indicate inner quartiles. Model results from BASE, NOSCAV, DEGAS DF10, and DEGAS DF20 simulations are shown with blue solid, black solid, black dashed, and black dotted lines, respectively. (b) Raw observational data of MSA in LFT, with color showing relative humidity (%). (c) Relative humidity and MSA concentrations anticorrelation in LFT. Blue dots represent raw data. Black dots represent flight averages, with bars indicating standard deviations. The red line represents a least squares regression of the observation data.

Since a full description of degassing entails detailed modeling of aerosols (e.g., composition, structure, acidity, efflorescence process, etc.), which is beyond the scope of this study, here we describe degassing with a simplified model that requires two parameters, an efflorescence point (EP) and a degassing fraction (DF). In the DEGAS simulation, we assign an EP of 40% (a value close to the EP of sea salt); a RH value of 40% also separates two clusters of high and low MSA observations during PASE (Figure 2c). We carry out a series of sensitivity simulations and determine the best estimate of DF to be 10–20%. Figure 2a shows that the DEGAS simulations with a 40% EP and a DF between 10% and 20% are able to bracket the observed median profile. More detailed simulation of the degassing mechanism requires more information on the microphysical property of PASE aerosols, which we do not currently have.

An alternative explanation of the LFT source relates to the long-range transport of MSA in the dry LFT. Previous studies have speculated that long-range transport contributes to SO_2 in the LFT [*Gray et al.*, 2011] and high cloud condensation nuclei concentrations [*Hudson and Noble*, 2009] during PASE. Back trajectory from the NOAA HYSPLIT model also suggests that the air mass in the LFT encountered in the PASE was advected from a

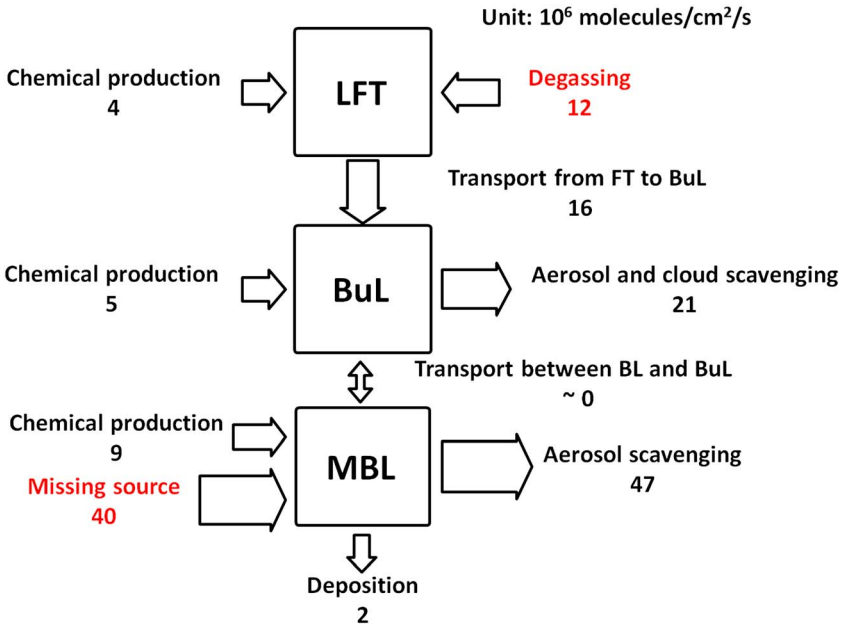

Figure 3. The budget of MSA in the MBL, the BuL, and the LFT.

©2014. American Geophysical Union. All Rights Reserved.

region with intensive biogenic activity over the East Pacific [*Gray et al*., 2011]. Although we are unable to simulate long-range transport because of the limitation of the 1-D model, observational evidence suggests that long-range transport is unlikely a major contributor to the enhancement of MSA in the LFT. The sharp increase of MSA from 1500 to 2000 m is inconsistent with a uniform vertical distribution of SO_2 as result of advection and vertical transport [*Gray et al*., 2011]. In addition, we cannot find a positive correlation between MSA and SO_2 if long-range transport is significant. In contrast, observations show a negative correlation between MSA and SO_2 in the LFT (Figure S6a in the supporting information). Furthermore, relative humidity is negatively correlated with MSA (Figure 2c) but is positively correlated with SO_2 (Figure S6b in the supporting information) in the LFT. These relationships are all consistent with degassing MSA in the LFT under dry conditions.

3.3. MSA Budget and Implications

Figure 3 summarizes the MSA budget in the MBL, the BuL, and the LFT, with a focus on required sources to explain the observations in the MBL and the LFT. In the MBL, we identify a missing source of 4.0×10^7 molecules/cm^2/s from the ocean surface. In contrast, chemical production from DMS oxidation constitutes only 9.0×10^6 molecules/cm^2/s on a daily basis. For sinks, dry deposition (2.0×10^6 molecules/cm^2/s) is small relative to the missing source. The dominant sink in the MBL is aerosol scavenging (4.7×10^7 molecules/cm^2/s). However, since the strength of aerosol scavenging varies little with altitude in the MBL (Figure S7 in the supporting information), the missing source from the surface is manifested by the observed negative concentration gradient in the MBL. In the LFT, degassing from aerosols constitutes an important source of 1.2×10^7 molecules/cm^2/s. The strength of chemical production in the LFT is 2.0×10^6 molecules/cm^2/s on a daily basis. Unlike in the MBL, the sink of aerosol scavenging is negligible owing to dry conditions in the LFT. The sole significant sink in the LFT is transport to the BuL, which is estimated at 1.6×10^7 molecules/cm^2/s. The total source strength in the LFT, the sum of degassing and chemical production, is much less than that in the MBL, but the weak sink and thus a long lifetime implies a much higher concentration of MSA in the LFT.

The budget of MSA highlights the missing surface source in the MBL and the degassing source in the LFT. Previous studies indicate that our knowledge of oceanic sulfur sources may be incomplete. For example, *Bandy et al*. [2011] suggested that the discrepancy in DMS-to-SO_2 conversion efficiency from two PASE studies [*Gray et al*., 2011; *Faloona et al*., 2009] can be reconciled if an additional oceanic sulfur source, half as strong as the DMS source, is present. The additional surface MSA source found here is only 2% of the DMS source during PASE, thus it is insufficient to reconcile the discrepancy. However, this MSA source may represent a group of organic sulfur compounds that have significant oceanic sources. If true, it would have significant implications to the marine sulfur budget and climate feedbacks over the tropical ocean. Model sensitivity analysis indicates that halogen (~1 pptv of BrO) oxidation of DMS is not a major contributor to MSA but MSA directly emitted or chemically produced could be important. Concurrent DMSO and MSA measurements will be necessary to constrain the model simulations presented here.

This study suggests that aerosols can act as a source of MSA under dry conditions (e.g., the LFT in the PASE). We note that the net transport between the MBL and BuL is negligible (Figure 3), indicating that gas phase MSA above the MBL is almost exclusively due to degassing from the aerosol phase. In addition, degassed MSA is not only MSA that aerosols scavenged elsewhere but also MSA produced from DMSO and MSIA in the aerosol phase [*Davis et al*., 1999; *Zhu et al*., 2006]. Therefore, the degassing source of MSA greatly enhances the apparent DMS-to-MSA conversion efficiency, which is quite small if only gas phase chemistry is accounted for. Furthermore, after transporting to humid and/or cold regions, these MSA gases may become an important contributor to new particle formation in the free troposphere [*Hoppel*, 1987]. For example, *Froyd et al*. [2009] reported previously that the enhancement of MSA/(MSA + sulfate) to ~0.5 in the aerosol phase in the upper free troposphere is accompanied by frequent formation of new particles (50% of flight time) over the tropical Pacific Ocean.

Our results suggest that degassing from dehydrated aerosols of soluble compounds like MSA could potentially provide important precursors for new particle formation in the free troposphere over the tropics, affecting the climate system through aerosol-cloud interactions. More broadly, we propose that aerosols may be an important media for transporting a suite of (sulfur or other) soluble compounds from the marine boundary layer to the free troposphere through the degassing mechanism. The potential for new particle formation from these soluble gases and the resulting climate forcing in the tropics will require targeted field experiments and modeling analysis to address.

©2014. American Geophysical Union. All Rights Reserved.

Acknowledgments
This work was supported by the NSF Atmospheric Chemistry Program. We thank an anonymous reviewer and the Editor for comments and suggestions that improved this paper. The data for this paper are available at the NCAR Earth Observing Laboratory (www.eol.ucar.edu/field_projects/pase).

The Editor thanks Stephen Conley for his assistance in evaluating this paper.

References

Bandy, A., D. C. Thornton, B. W. Blomquist, S. Chen, T. P. Wade, J. C. Ianni, G. M. Mitchell, and W. Nadler (1996), Chemistry of dimethyl sulfide in the equatorial Pacific atmosphere, *Geophys. Res. Lett.*, *23*(7), 741–744, doi:10.1029/96GL00779.

Bandy, A., et al. (2011), Pacific Atmospheric Sulfur Experiment (PASE): Dynamics and chemistry of the south Pacific tropical trade wind regime, *J. Atmos. Chem.*, *68*(1), 5–25.

Bandy, A. R., D. C. Thornton, F. H. Tu, B. W. Blomquist, W. Nadler, G. M. Mitchell, and D. H. Lenschow (2002), Determination of the vertical flux of dimethyl sulfide by eddy correlation and atmospheric pressure ionization mass spectrometry (APIMS), *J. Geophys. Res.*, *107*(D24), 4743, doi:10.1029/2002JD002472.

Barnard, W. R., M. O. Andreae, W. E. Watkins, H. Bingemer, and H. W. Georgii (1982), The flux of dimethylsulfide from the oceans to the atmosphere, *J. Geophys. Res.*, *87*(NC11), 8787–8793, doi:10.1029/JC087iC11p08787.

Charlson, R. J., J. E. Lovelock, M. O. Andreae, and S. G. Warren (1987), Oceanic phytoplankton, atmospheric sulfur, cloud albedo and climate, *Nature*, *326*(6114), 655–661.

Chen, G., D. D. Davis, P. Kasibhatla, A. R. Bandy, D. C. Thornton, B. J. Huebert, A. D. Clarke, and B. W. Blomquist (2000), A study of DMS oxidation in the tropics: Comparison of Christmas Island field observations of DMS, SO_2, and DMSO with model simulations, *J. Atmos. Chem.*, *37*(2), 137–160.

Clarke, A. D., et al. (2004), Size distributions and mixtures of dust and black carbon aerosol in Asian outflow: Physiochemistry and optical properties, *J. Geophys. Res.*, *109*, D15S09, doi:10.1029/2003JD004378.

Conley, S. A., I. Faloona, G. H. Miller, D. H. Lenschow, B. Blomquist, and A. Bandy (2009), Closing the dimethyl sulfide budget in the tropical marine boundary layer during the Pacific Atmospheric Sulfur Experiment, *Atmos. Chem. Phys.*, *9*(22), 8745–8756.

Covington, A. K., R. A. Robinson, and R. Thompson (1973), Osmotic and activity coefficients for aqueous methane sulfonic acid solutions at 25. deg, *J. Chem. Eng. Data*, *18*(4), 422–423.

Davis, D., G. Chen, P. Kasibhatla, A. Jefferson, D. Tanner, F. Eisele, D. Lenschow, W. Neff, and H. Berresheim (1998), DMS oxidation in the Antarctic marine boundary layer: Comparison of model simulations and held observations of DMS, DMSO, $DMSO_2$, H_2SO_4(g), MSA(g), and MSA(p), *J. Geophys. Res.*, *103*(D1), 1657–1678, doi:10.1029/97JD03452.

Davis, D., et al. (1999), Dimethyl sulfide oxidation in the equatorial Pacific: Comparison of model simulations with field observations for DMS, SO_2, H_2SO_4(g), MSA(g), MS, and NSS, *J. Geophys. Res.*, *104*(D5), 5765–5784, doi:10.1029/1998JD100002.

Faloona, I., S. A. Conley, B. Blomquist, A. D. Clarke, V. Kapustin, S. Howell, D. H. Lenschow, and A. R. Bandy (2009), Sulfur dioxide in the tropical marine boundary layer: Dry deposition and heterogeneous oxidation observed during the Pacific Atmospheric Sulfur Experiment, *J. Atmos. Chem.*, *63*(1), 13–32.

Froyd, K. D., D. M. Murphy, T. J. Sanford, D. S. Thomson, J. C. Wilson, L. Pfister, and L. Lait (2009), Aerosol composition of the tropical upper troposphere, *Atmos. Chem. Phys.*, *9*(13), 4363–4385.

Gray, B. A., Y. Wang, D. Gu, A. Bandy, L. Mauldin, A. Clarke, B. Alexander, and D. D. Davis (2011), Sources, transport, and sinks of SO_2 over the equatorial Pacific during the Pacific Atmospheric Sulfur Experiment, *J. Atmos. Chem.*, *68*(1), 27–53.

Hoppel, W. A. (1987), Nucleation in the MSA water-vapor system, *Atmos. Environ.*, *21*(12), 2703–2709.

Hudson, J. G., and S. Noble (2009), CCN and cloud droplet concentrations at a remote ocean site, *Geophys. Res. Lett.*, *36*, L13812, doi:10.1029/2009GL038465.

Liu, Z., et al. (2010), Evidence of reactive aromatics as a major source of peroxy acetyl nitrate over China, *Environ. Sci. Technol.*, *44*(18), 7017–7022.

Liu, Z., et al. (2012), Summertime photochemistry during CAREBeijing-2007: RO_x budgets and O_3 formation, *Atmos. Chem. Phys.*, *12*(16), 7737–7752.

Mauldin, R. L., G. J. Frost, G. Chen, D. J. Tanner, A. S. H. Prevot, D. D. Davis, and F. L. Eisele (1998), OH measurements during the First Aerosol Characterization Experiment (ACE 1): Observations and model comparisons, *J. Geophys. Res.*, *103*(D13), 16,713–16,729, doi:10.1029/98JD00882.

Mauldin, R. L., D. J. Tanner, J. A. Heath, B. J. Huebert, and F. L. Eisele (1999), Observations of H_2SO_4 and MSA during PEM-Tropics-A, *J. Geophys. Res.*, *104*(D5), 5801–5816, doi:10.1029/98JD02612.

Nowak, J. B., et al. (2001), Airborne observations of DMSO, DMS, and OH at marine tropical latitudes, *Geophys. Res. Lett.*, *28*(11), 2201–2204, doi:10.1029/2000GL012297.

Ridley, B. A., F. E. Grahek, and J. G. Walega (1992), A small, high-sensitivity, medium-response ozone detector suitable for measurements from light aircraft, *J. Atmos. Oceanic Tech.*, *9*(2), 142–148.

Wang, Y., et al. (2001), Factors controlling tropospheric O_3, OH, NO_x and SO_2 over the tropical Pacific during PEM-Tropics B, *J. Geophys. Res.*, *106*(D23), 32,733–32,747, doi:10.1029/2001JD900084.

Wang, Y., Y. Choi, T. Zeng, D. Davis, M. Buhr, G. Huey, and W. Neff (2007), Assessing the photochemical impact of snow NO_x emissions over Antarctica during ANTCI 2003, *Atmos. Environ.*, *41*(19), 3944–3958.

Weber, R. J., K. Moore, V. Kapustin, A. Clarke, R. L. Mauldin, E. Kosciuch, C. Cantrell, F. Eisele, B. Anderson, and L. Thornhill (2001), Nucleation in the equatorial Pacific during PEM-Tropics B: Enhanced boundary layer H_2SO_4 with no particle production, *J. Geophys. Res.*, *106*(D23), 32,767–32,776, doi:10.1029/2001JD900250.

Zhu, L., A. Nenes, P. H. Wine, and J. M. Nicovich (2006), Effects of aqueous organosulfur chemistry on particulate methanesulfonate to non-sea salt sulfate ratios in the marine atmosphere, *J. Geophys. Res.*, *111*, D05316, doi:10.1029/2009GL038465.

©2014. American Geophysical Union. All Rights Reserved.